VOL. 9, NO. 12, DECEMBER 2014 ISSN 1819-6608
ARPN Journal of Engineering and Applied Sciences


www.arpnjournals.com

EFFECTS OF CHEMICAL REACTION AND HEAT GENERATION ON A MIXED CONVECTION STAGNATION POINT FLOW, HEAT AND MASS TRANSFER TOWARDS A STRETCHING VERTICAL POROUS FLAT PLATE

A. Adeniyan and C. S. Ogwuegbu
Department of Mathematics, University of Lagos, Lagos, Nigeria
E-Mail: aadeniyan@unilag.edu.ng

ABSTRACT

This study investigates a two-dimensional steady boundary layer stagnation laminar flow of heat and mass transfer due to a viscous, incompressible and first-order homogeneous chemically reacting fluid towards a heated stretching porous vertical plate embedded in a Newtonian fluid. The basic governing flow partial differential equations together with the boundary conditions are converted into a set of ordinary differential equations by means of existing similarity variables. The transformed set of equations were solved numerically by assigning realistic values to the basic flow parameters, using the classical Runge-Kutta fourth order integration method along with a shooting technique and implemented on Maple software. Important engineering dimensionless quantities of interest such as the wall shear stress, heat and mass transfer rates are analyzed, and discussed by means of graphs and tables. In other to ascertain the credibility of our computed results, comparisons were made with the existing, available and open literature works and have been found to be in extremely good agreement.

Keywords: chemical reaction, internal heat generation, mixed convection, stretching pervious surface, stagnation flow.

1. INTRODUCTION

The study on the flow, heat and mass transfer near a stagnation point has become increasingly important and has attracted the attention of several researchers in recent past years due to its broad applications in industrial and technological processes such as the cooling of an electronic device by fans, cooling of nuclear reactors in the case of unscheduled switch-off, fiber technology and extrusion processes. Hiemenz [1] was the first to study the two dimensional stagnation point flow, and obtained exact similarity solutions of the governing momentum equations. Since then many researchers have considered other aspects of such flows and obtained closed-form analytically as well as numerical solutions. To mention but a few, Ramachandram *et al*. [2] studied laminar mixed convection in two dimensional stagnation flow around heated surfaces by considering both cases of an arbitrary wall temperature and arbitrary surface heat flow variations. They found that a reverse flow developed in the buoyancy opposing flow regions and dual solutions are found to exist for a certain range of the buoyancy parameter. This work has then extended by Devi *et al*. [3] for the unsteady case regime. Heat transfer or heat and mass problems over a pervious surface have been examined by Gupta and Gupta [4], Magyari and Keller [5], Ibrahim and Makinde [6]. Mixed convection problems become very relevant when the influence of gravitational fields becomes consequential and noticeable on the fluid films near the solid boundary. In such cases the ambient fluid velocity may not be too strong and the thermal and solutal differences between the moving surface and the far field fluid are realistically large such that buoyant forces influence on forced convective heat and mass transfer intensifies. In industrial applications, the stretched surface speed and temperature play significant role in the cooling processes. For example, during the industrial manufacturing of metallic, plastic and rubber sheets, it is often necessary to blow a gaseous medium through a yet to be solidified material. The study of flow and heat transfer is exemplified for determining the top-most quality of the final products, most especially by controlling the surface temperature and accompanies environmental conditions. Of recent, Okedayo *et al*. [7], Aman *et al*. [8] considered the case of a mixed convection MHD with convective boundary conditions. Makinde and Olanrewaju [9] examined the unsteadiness, chemical reaction, Soret and Dufour effects for a mixed convection flow over permeable plate moving through a binary mixture which may be regarded as an extension of Makinde *et al*. [10], devoid of thermal radiation characteristics. Olarewaju and Gbadeyan [11] considered a two-dimentional case with Soret, Dufour, chemical reaction, thermal radiation and heat generation/absorption effects for a mixed convection flow in porous media. Olanrewaju and Adeniyan [12], who presented a numerical investigation through a shooting method, for the thermal-diffusion and diffusion-thermo effects with thermal radiation on a two-dimensional steady flow, heat and mass transfer due to a moving vertical plate placed in a porous medium. In their analysis it was pointed out that for some specific mixtures such as hydrogen-air with light and medium molecular weight, Dufour and Soret effects play a significant role in industrial processes requiring isotope separation. The stagnation point flow towards a surface which is moved or stretched has been considered by Chaim [13], Ishak *et al*. [14, 15]. Without a controversy, it has been shown by many a researcher such as Ridha [16], Merkin and Pop [17], Aman and Ishak [18],

Bachok *et al*. [19], that dual solutions exist not only in the case for which the mixed buoyancy parameter is negative but also when it is positive. Our research is centered on cooling problems in engineering and industrial processes, where the positive mixed convection parameter is of relevance (see Makinde and Olanrewaju [20] consequent upon the choice of the latter, we extend the work by Ishak *et al*. [15] for the case of a first order homogeneous chemically reacting fluid flow, with heat generation over a stretching pervious surface.

In section 2 we present problem formulation and basic equations, section 3 accounts for the numerical procedure, section 4 concerns with results and discussion while section 5 reports the conclusions.

2. PROBLEM FORMULATION AND BASIC EQUATIONS

We considered a two-dimensional steady stagnation point flow of a chemically reactive incompressible viscous fluid perpendicular to a vertical plate which is immersed in it. It is assumed that the ambient fluid is moving with a velocity $u_e(x) = {}_{Ue}x$ in the y-direction towards the stagnation point on the plate, where ${}_{Ue}$ is a non-negative constant with unit (time)$^{-1}$. It is also assumed that the surface is stretched in the x-direction such that the x-component of the velocity, temperature and concentration vary linearly along the plate from stagnation point, that is,

$$u_w(x) = U_w x, \qquad T_w(x) = T_\infty + T_0 x \text{ and } C_w(x) = C_\infty + C_0 x ,$$

where U_w is a positive constant with unit (time)$^{-1}$, T_0 and C_0 are arbitrary constants with units temperature per distance and concentration per distance respectively, while T_∞ and C_∞ are respective ambient fluid temperature and concentration. Under these assumptions along with Boussinesq and boundary layer approximations, the equations which model the boundary layer flow are given by

$$\frac{\partial u}{\partial x} + \frac{\partial v}{\partial y} = 0 \tag{1}$$

$$u\frac{\partial u}{\partial x} + v\frac{\partial u}{\partial y} = U_e\frac{dU_e}{dx} + \nu\frac{\partial^2 u}{\partial y^2} + g[\beta(T - T_\infty) + \beta_c(C - C_\infty)] \tag{2}$$

$$u\frac{\partial T}{\partial x} + v\frac{\partial T}{\partial y} = \alpha\frac{\partial^2 T}{\partial y^2} + \frac{Q_0(T - T_\infty)}{\rho c_p} \tag{3}$$

$$u\frac{\partial C}{\partial x} + v\frac{\partial C}{\partial y} = D_m\frac{\partial^2 C}{\partial y^2} - K_r(C - C_\infty) \tag{4}$$

and subject to the boundary conditions:

$$\left.\begin{array}{l} v = V_w, u = u_w(x), \quad T = T_w(x), \quad C = C_w(x) \text{ at } y = 0 \\ u \to u_e(x), \quad T \to T_\infty, \quad C \to C_\infty \text{ (x) as } y \to \infty. \end{array}\right\} \tag{5}$$

In the above equations (2.1) – (2.5), the velocity field is (u(x, y), v(x, y)) where u and v are the components of the velocity along the x and y axes respectively. T being the temperature field and g being the gravitational acceleration, $\alpha\left(= \frac{\kappa Q_0}{k}\right)$, ν, β β_c are the thermal diffusivity, kinematic viscosity, thermal and concentration expansion coefficients respectively. The last two terms within the brackets in (2) represent the thermal and the concentration buoyancy forces respectively. $V_w(x)$ is the mass flux at the wall characterized respectively as mass withdrawal or suction and mass blowing or injection depending on whether or not Fw is strictly greater than or less than zero. Q_0 is the volumetric internal heat energy generation, ρ is fluid density, k is thermal conductivity of the fluid, μ is the fluid dynamic viscosity and c_p is the specific heat at constant pressure, D_m is the coefficient of diffusivity due to mass transfer and K_r is the reaction rate constant of first-order chemical reaction.

Similarity variables / dimensionless parameters used in the transformation of equations (1)-(5) above are:

$$\lambda_t = \frac{g\beta T_0}{U_w^2}, \lambda_c = \frac{g\beta_c C_0}{U_w^2}, \varepsilon = \frac{U_e}{U_w}, \Pr = \frac{\mu c_p}{k}, \text{Sc} = \frac{\nu}{D_m}, S = \frac{Q_0}{\rho c_p U_w}, K = \frac{K_r}{U_w}, F_w = -\frac{V_w}{U_w} \tag{6}$$

In equation (6) above Pr is the Prandtl number, ε is the ratio of the velocity at wall to the velocity far off from the wall, λ_t is the thermal Grashof number while λ_c is the concentration Grashof number, S is the internal heat generation parameter, Sc is the Schmidt number and K is the reaction rate parameter, F_w is the dimensionless suction/injection parameter, ψ is the stream function whereas f is the dimensionless stream function. Fw>0 (or $V_w(x) < 0$) signifies suction, Fw<0 (or $V_w(x) > 0$) stands for injection, and of course Fw=0 (or $V_w(x) = 0$) demands that the plate be impervious or impermeable. Mentions are the cases for which $\varepsilon = 0, 0 < \varepsilon < 1$, $\varepsilon = 1$ and $\varepsilon > 1$ corresponding to when the plate stretches in an otherwise still fluid, when the free-stream is slower in speed as compared with the stretching plate, when the plate and the free-stream move with equal speed along the same direction and when the free-stream is faster in speed as compared with the stretching plate respectively. We are not considering cases for which $\varepsilon < 0$ designated for shrinking plate in this present study. It is noteworthy that our research interest is concerned with the case for which $\lambda_t > 0$ (corresponding to cooling problem), $\lambda_c > 0$ (indicating that the wall chemical species concentration is larger than that far from the wall) and S>0 (concerning internal heat source problem). Here again, we shall not consider the case for which the reaction rate parameter K<0 (corresponding to generative chemical reaction) but settle for K>0 (corresponding to destructive chemical reaction).

In terms of the dimensional stream function the velocity components are

$$u = \frac{\partial \psi}{\partial y}, v = -\frac{\partial \psi}{\partial x} \quad (7)$$

Equation (7) satisfies identically the continuity equation (1) and with the help of the similarity variables the momentum, energy and concentration equations are transformed into

$$f''' + ff'' - (f')^2 + \lambda_t \theta + \lambda_c \phi + \varepsilon^2 = 0 \quad (8)$$

$$\frac{1}{Pr}\theta'' + f\theta' - [(f)]' - S)\theta = 0 \quad (9)$$

$$\frac{1}{Sc}\phi'' + f\phi' - (f' + K)\phi = 0 \quad (10)$$

subject to the transformed boundary conditions:

$$\left.\begin{aligned} f(0) = Fw, \quad f'(0) = 1, \quad \theta(0) = 1, \quad \phi(0) = 1, \\ f'(\infty) \to \varepsilon, \quad \theta(\infty) \to 0, \quad \phi(\infty) \to 0, \end{aligned}\right\} \quad (11)$$

where the primes denote differentiation with respect to η.

The physical quantities of engineering interest are the local skin-friction coefficient C_F, the local Nusselt number Nu_x and the local Sherwood number Sh_x. These quatities may respectively be defined in terms of the surface shear stress τ_w, the surface heat flux q_w, and the surface mass flux q_m as

$$C_F = \frac{\tau_w}{\rho u_w^2}, \quad Nu_x = \frac{xq_w}{k[(T)_w - T_\infty)}, \quad Sh_x = \frac{xq_m}{D_m[(C)_w - C_\infty)}, \quad (12)$$

where

$$\tau_w = \mu\frac{\partial u}{\partial y}, \quad q_w = -k\frac{\partial T}{\partial y} \text{ and } q_m = -D_m\frac{\partial C}{\partial y} \text{ at } y = 0. \quad (13)$$

Upon the use of the transformations encompassed in (6), we find

$$C_F\sqrt{Re_x} = f''(0), \quad \frac{Nu_x}{\sqrt{Re_x}} = -\theta'(0) \text{ and } \frac{Sh_x}{\sqrt{Re_x}} = -\phi'(0) \quad (14)$$

where the local Reynolds number $Re_x = \frac{u_w x}{\nu} = \frac{U_w x^n}{\nu}$.

3. NUMERICAL PROCEDURE

The set of nonlinear coupled ordinary differential equations (8)-(10) and the transformed boundary conditions (11) have been reduced to an equivalent system of initial value problem (IVP) by means of a shooting technique and then solved numerically with meaningfully selected values of the basic flow parameters Pr, S, Fw, ε, λ_t, λ_c using a classical fourth order Runge-Kutta method via a computer program written in MAPLE - 14 version. Choice was made of appropriate finite value of η_∞ and a step size of $\Delta\eta = 10^{-3}$ has been satisfactorily made use of, to meet up a convergence criterion of 10^{-7} in nearly all cases. Also for each iteration loop, the far field transverse distance from the plate, y_∞ has been obtained computationally through the assignment $\eta = \eta_\infty + \Delta\eta$. The maximum value of η_∞, to each group of the basic parameters has been computed when the values of unknown boundary conditions at η = 0 do not change to successful loop with error less than 10^{-7} ensuring no do-loop and critical point.

4. RESULTS AND DISCUSSIONS

The influence of the various governing flow parameters are examined and sorted out numerically on the flow, heat and mass transfer characteristics of this present study. The accuracy of this numerical method was validated by direct comparison with the numerical results reported in the literature by Ishak *et al*. [15] excluding the concentration equation and the internal heat generation or absorption. As demonstrated in Tables 1 and 2, a perfect agreement has been achieved.

Table-1. Computations showing comparison with Ishak *et al*. [15] results for $S = \lambda_c = Sc = K = F_W = 0$.

ε	λ_t	Pr	$f''(0)$ Ishak et al. [15]	$f''(0)$ Present study
0	-0.1	1	-1.0513	-1.051348
0.01	-0.1	1	-1.0490	-1.049001
0.2	-0.1	1	-0.9638	-0.963836
0.1	1	1	-0.5398	-0.539841
1	10	1	2.9495	2.949430
5	10	1	13.6462	13.645738

4.1. Computational results

The results illustrate the influence of the thermal Grashof number (λ_t), solutal Grashof number (λ_c), prandtl number (Pr), Schmidt number (Sc), velocity ratio (ε), internal heat generation (S), suction or injection parameter (F_w) not only on the skin friction but also on the rates of heat and mass transfer at the plate surface. The value of Pr is taken to vary between 0.71 and 7.1 which corresponds to air and water respectively.

Table-2 shows the numerical results for various basic flow parameter variations. It is observed that the magnitude of the Skin- friction coefficient at the surface of the plate or its absolute value increases with Prandtl number (Pr), internal heat generation parameter (S), thermal and solutal Grashof numbers (λ_t, λ_c), reaction rate parameter (K) and suction(Fw>0) and Sc in absolute values, but decreases with the dimensionless injection (Fw<0). Considering the Skin friction $f''(0)$, the Nusselt number $-\theta'(0)$, and the local Sherwood number $|\phi(0)$, it was noticed that each of these fluid characteristics increased with increase in either of λ_t, λ_c K or Sc. However, $f''(0)$, and $-\theta'(0)$ increased with S, but $|\phi'(0)$ was decreased with S increasing. The influence of Sc on either of $-\theta'(0)$ and $|\phi'(0)$ produced increment in their values. One observed in the $f''(0)$ column of this Table alternating values depending on the parameter variations and the range of values of the varying dimensionless parameters. The negative values of $f''(0)$ signify that the stretching plate exerts a drag force on the fluid while positive values manifest the reverse. As revealed in Table-3, again $f''(0)$ appreciated in values as the velocity ratio ε varied from 0.1 to 0.5, but $-\theta'(0)$ and $|\phi'(0)$ depreciated in values.

Table-2. Computations showing the results of variation of basic flow parameters on $f''(0)$, $-\theta'(0)$ and $|\phi'(0)$.

Pr	S	ε	λ_C	λ_t	K	F_W	Sc	$f''(0)$	$-\theta'(0)$	$-\phi'(0)$
0.72	1.0	0.05	0.5	0.5	0.2	0.5	0.24	-0.362235	0.353531	0.639325
1.00	1.0	0.05	0.5	0.5	0.2	0.5	0.24	-0.608409	0.754551	0.595322
7.10	1.0	0.05	0.5	0.5	0.2	0.5	0.24	-0.803678	5.461015	0.575853
0.72	1.5	0.05	0.5	0.5	0.2	0.5	0.24	0.143721	3.312049	0.704307
0.72	2.0	0.05	0.5	0.5	0.2	0.5	0.24	0.788334	8.237802	0.687999
0.72	1.0	0.10	0.5	0.5	0.2	0.5	0.24	0.371568	0.281466	0.637857
0.72	1.0	0.50	0.5	0.5	0.2	0.5	0.24	0.266030	0.484058	0.657451
0.72	1.0	0.05	2.0	0.5	0.2	0.5	0.24	0.265661	0.475912	0.669853
0.72	1.0	0.05	5.0	0.5	0.2	0.5	0.24	1.599136	0.849068	0.741891
0.72	1.0	0.05	0.5	2.0	0.2	0.5	0.24	0.309152	0.465426	0.672296
0.72	1.0	0.05	0.5	4.0	0.2	0.5	0.24	1.097500	0.689579	0.705357
0.72	1.0	0.05	0.5	0.5	0.4	0.5	0.24	0.361390	0.391573	0.683357
0.72	1.0	0.05	0.5	0.5	1.0	0.5	0.24	0.362457	0.465470	0.796491
0.72	1.0	0.05	0.5	0.5	0.2	-2.0	0.24	0.000645	0.380873	0.420081
0.72	1.0	0.05	0.5	0.5	0.2	-1.0	0.24	-0.004232	0.602472	0.510207
0.72	1.0	0.05	0.5	0.5	0.2	0.0	0.24	-0.159734	0.588108	0.598605
0.72	1.0	0.05	0.5	0.5	0.2	1.0	0.24	-0.688693	0.103566	0.677795
0.72	1.0	0.05	0.5	0.5	0.2	2.0	0.24	-1.578829	1.210323	0.781021
0.72	1.0	0.05	0.5	0.5	0.2	0.5	0.64	-0.380232	0.610947	1.176299
0.72	1.0	0.05	0.5	0.5	0.2	0.5	0.78	-0.389183	0.635854	1.329751

4.2. Effect of parameter variation on velocity, temperature and concentration profiles

4.2.1. Velocity profiles

The effects of various parameters on velocity profiles in the boundary layer region are clearly shown in Figures 1 to 7 and the variation of each of the governing parameters listed in the Figure legends. It is observed in Figures 1 to 6 that the dimensionless velocity starts from a maximum value of 1 at the plate surface and decreases monotonically to a quiescent free stream value located for away from the plate surface for fixed = 0.05, thereby satisfying the far field boundary conditions for all other parameter variations. Figures 2, 3 and 4 show an increase in velocity when the internal heat generation, the thermal Grashof number as well as the solutal Grashof is increased near the plate, but the velocity boundary layer thickness is seen to get thinner in the case of Figure-1 as the Prandtl number appreciates from the values for air to that of water and the velocity overshoots noticed near the plates. An increase in velocity observed in Figure-4 does not reflect significant influence on the thickness of the velocity boundary layer as the solutal Grashof number strengthens. Figure-3 depicts the variation of the velocity profiles with the velocity ratio. Here the dimensionless velocity increases as increases with wall unit value to far field value and overshoots near the plate for . The velocity profiles intensify as thermal Grashof number progresses, up to about two fifth of the transverse distance from the plate in Figure-5, after which there is a crossover and the velocity decreases as increases. Figure-6 shows both a decrease in velocity and the velocity boundary layer thickness as more fluid is slowly sucked away from the fluid regime while the reverse is observed as more fluid is injected into the flow for fixed values of other flow parameters. This observation clearly conforms to those of Makinde *et al*. [21]. Interestingly, mass suction can be used as a means of stabilizing liquid film flow adjacent to a stretching plate, a relevant demand for industrial plate coating to minimize wastage and thus reduce production cost.

Figure-7 depicts the velocity profiles for various values of for respective fixed injection and suction with all other parameters unvarying. It is observed that when the flow velocity due to suction leads that of the injection in contrast to the results when . Furthermore, Figure-7 shows that when there occurs an inversion of flow near the stretching plate and the boundary layer thickness becomes thinner with an increase in .

4.2.2. Temperature profiles

The influences of various embedded parameters on the fluid temperature are illustrated in Figures 8 to 15 and the range of each parameter variations indicated in the Figure legends. An overshoot in temperature has been observed due to alteration of the parameters and at the plate surface or far from it the boundary conditions are fulfilled. Again this serves as a further confirmation of our numerical integration codes. As indicated in Figures 8 and 9 to 12, the dimensionless fluid temperature falls consequential upon increment in each of the parameters Pr, , , is increased while the reverse has been observed in Figures 13 and 14, in which the temperature is seen to increase respectively with chemical reaction parameter and Schmidt number but abysmal effects on the thermal boundary layer thickness prevail. In Figure-15 two important revelations have been observed. Firstly, fluid becomes hotter as mass blowing (injection) intensifies in strength. Secondly one sees that as fluid withdrawal (injection) persists increasingly, the fluid temperature diminishes in value, consequential upon thinning of the thermal boundary layer thickness while other basic flow parameters remained unaltered. It lends itself to a conjecture, therefore that suction may serve as a means of temperature control for the process of cooling, the much needed factor in the industrial production of some materials such as aerodynamic extrusion of metallic and plastic plates, etc let aside the usual physically accepted norms of use of Prandtl, positive thermal and solutal Grashof numbers (see Makinde and Olanrewaju [9]. It is reported in Figure-24 that, for fixed values of other flow governing parameters, the concentration is larger for mass blowing (injection) as compared with that of mass withdrawal (suction) for all cases of the values of the velocity ratio , where =(value)+ and =(value)- signify respectively the suction and the injection.

4.2.3. Concentration profiles

The effects of various thermo-physical parameters on the fluid concentration are illustrated in Figures 16 to 24 indicating full compliance with the boundary conditions (2.11) as the concentration is seen to peak at the plate surface with a value of 1.0 and then diminishes exponential decrease to minimum value (zero) at the far from the plate. Figures 16 and 23 (upper profiles) show an increase in the concentration boundary layer thickness for an increase in the Prandtl number and injection parameter respectively for the range of values indicated in the Figure legends while other basic flow parameters remain fixed but Figures 17 to 23 (lower profiles) all show the contrary. As the parameter in each of these figure legends increases a discernible decrease in the concentration profiles is noticed. Not only the thermal heat generation parameter (S) induces a diminution in the concentration but also the solutal Grashof number, the Schmidt number, the velocity ratio, the chemical reaction and the suction parameters.

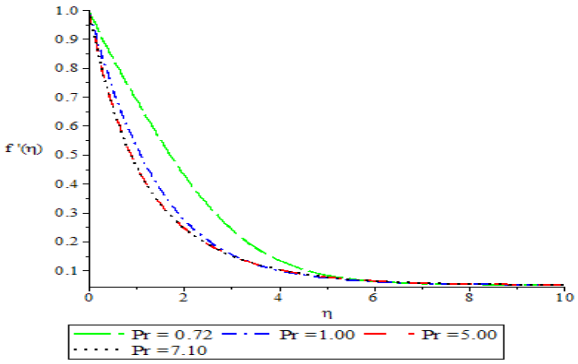

Figure-1. Velocity profiles for
$S = 1.0, \varepsilon = 0.05, \lambda_t = 0.5, \lambda_C = 0.5, K = 0.2, F_W = 0.5, Sc = 0.24$.

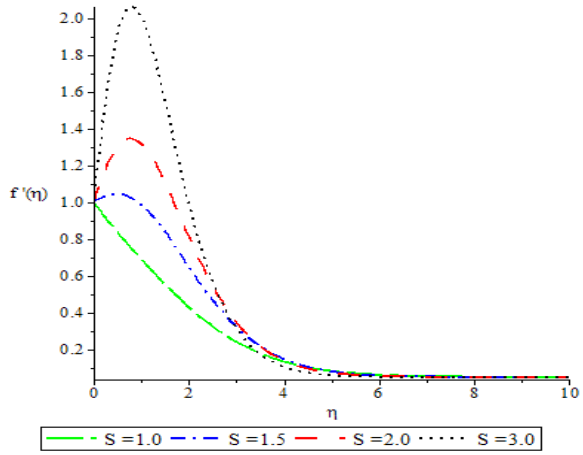

Figure-2. Velocity profiles for
$Pr = 0.72, \varepsilon = 0.05, \lambda_t = 0.5, \lambda_C = 0.5, K = 0.2, F_W = 0.5, Sc = 0.24$.

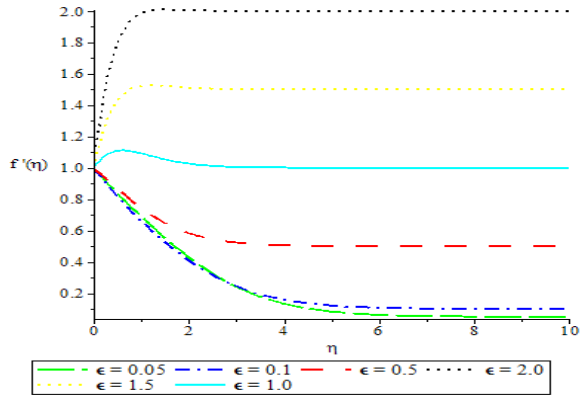

Figure-3. Velocity profiles for
$Pr = 0.72, S = 1.0, \lambda_t = 0.5, \lambda_C = 0.5, K = 0.2, F_W = 0.5, Sc = 0.24$.

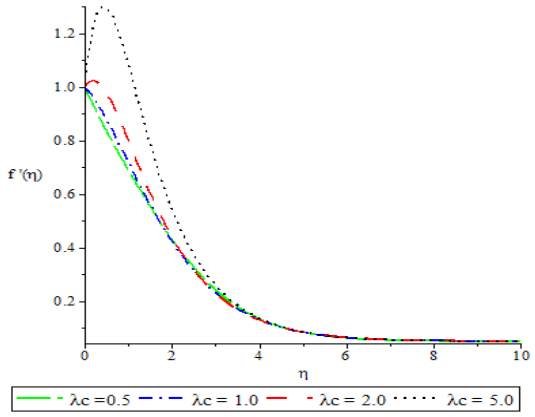

Figure-4. Velocity profiles for
$Pr = 0.72, S = 1.0, \varepsilon = 0.05, \lambda_t = 0.5, K = 0.2, F_W = 0.5, Sc = 0.24$.

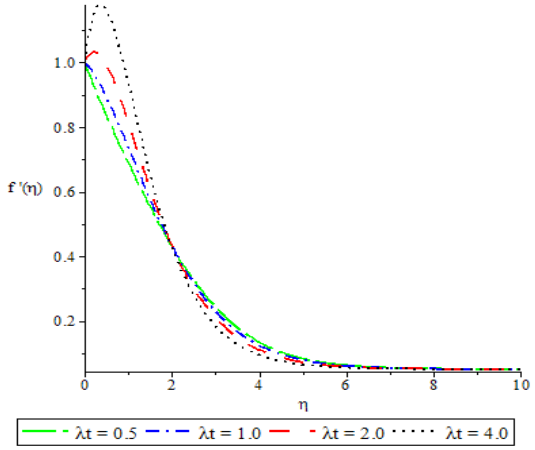

Figure-5. Velocity profiles for
$Pr = 0.72, S = 1.0, \varepsilon = 0.05, \lambda_C = 0.5, K = 0.2, F_W = 0.5, Sc = 0.24$.

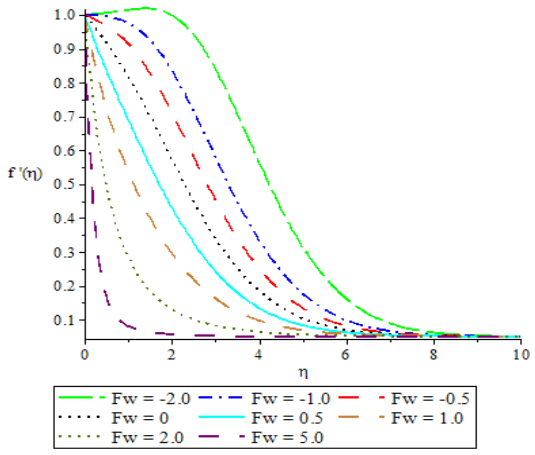

Figure-6. Velocity profiles showing the influence of suction/injection for
$Pr = 0.72, S = 1.0, \varepsilon = 0.05, \lambda_t = 0.5, \lambda_C = 0.5, K = 0.2, Sc = 0.24$.

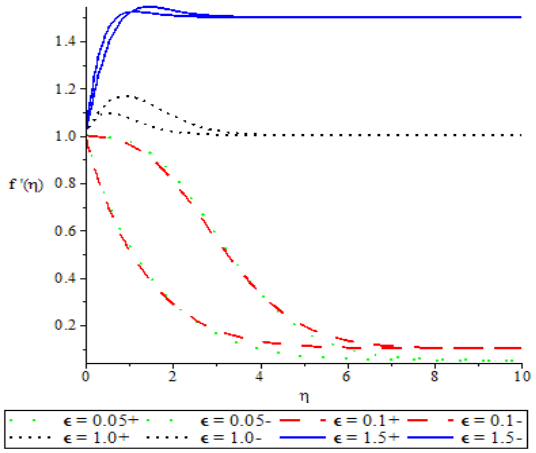

Figure-7. Velocity profiles for
$Pr = 0.72,\ S = 1.0, \lambda_t = 0.5, \lambda_c = 0.5, K = 0.2, Sc = 0.24,\ F_W = -\frac{1.0}{1.0}$.

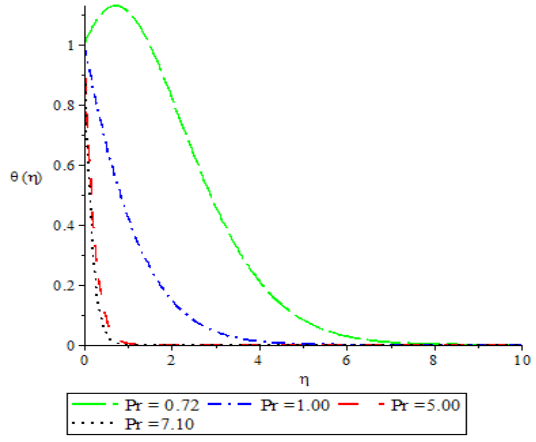

Figure-8. Temperature profiles for
$S = 1.0, \varepsilon = 0.05, \lambda_t = 0.5, \lambda_c = 0.5, K = 0.2, F_W = 0.5, Sc = 0.24$.

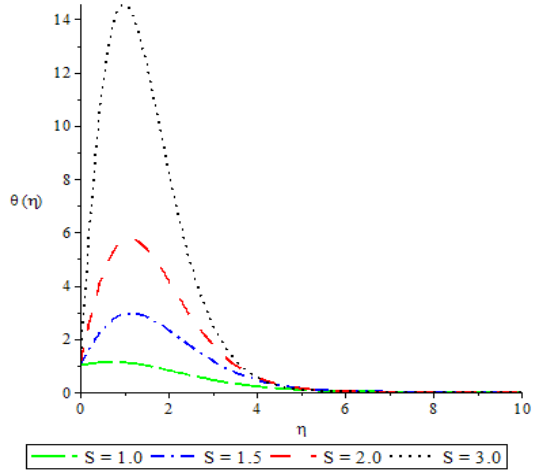

Figure-9. Temperature profiles for
$Pr = 0.72,\ \varepsilon = 0.05, \lambda_t = 0.5, \lambda_c = 0.5, K = 0.2, F_W = 0.5, Sc = 0.24$.

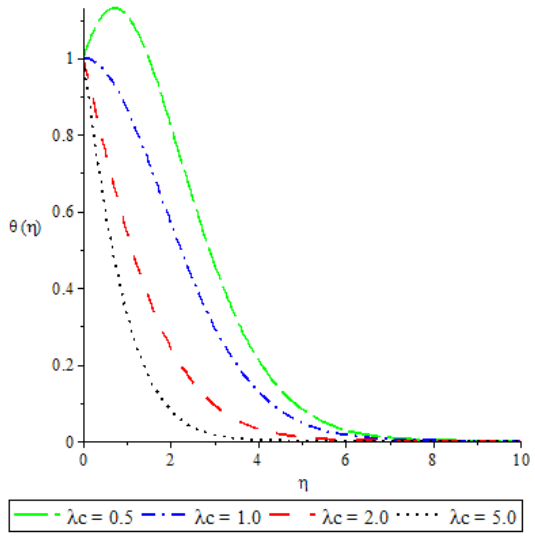

Figure-10. Temperature profiles for
$Pr = 0.72,\ S = 1.0, \varepsilon = 0.05, \lambda_t = 0.5, K = 0.2, F_W = 0.5, Sc = 0.24$.

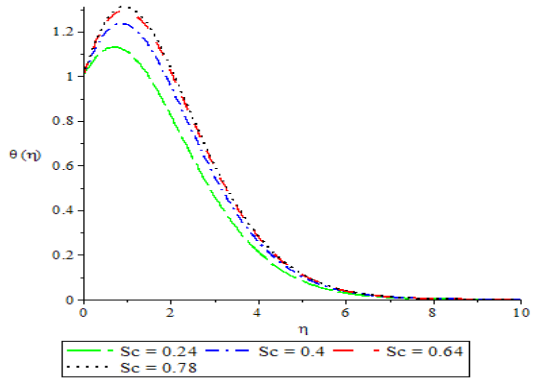

Figure-14. Temperature profiles for
$Pr = 0.72,\ S = 1.0, \varepsilon = 0.05, \lambda_t = 0.5, \lambda_c = 0.5, K = 0.2, F_W = 0.5$.

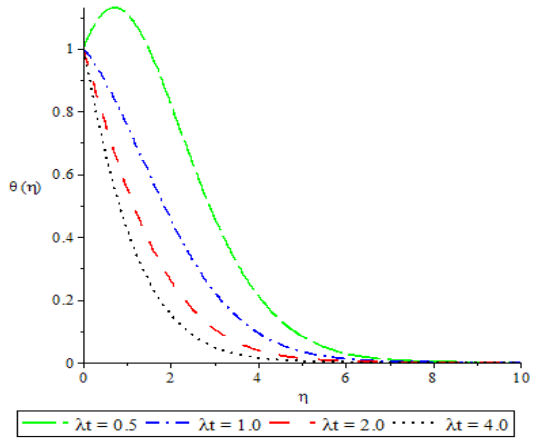

Figure-11. Temperature profiles for
$Pr = 0.72,\ S = 1.0, \varepsilon = 0.05,\ \lambda_c = 0.5, K = 0.2, F_W = 0.5, Sc = 0.24$.

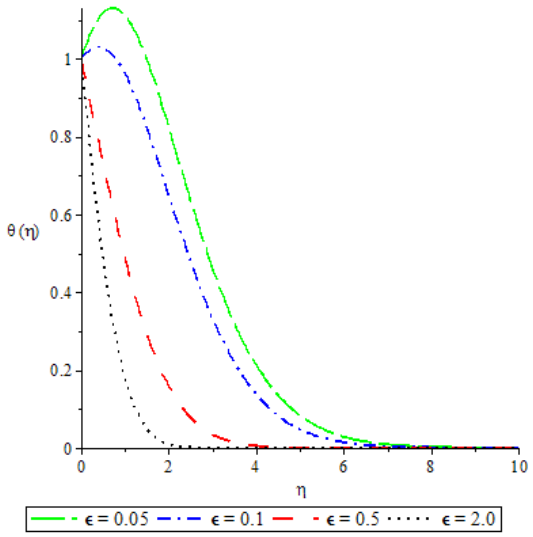

Figure-12. Temperature profiles for
$Pr = 0.72,\ S = 1.0, \lambda_t = 0.5, \lambda_C = 0.5, K = 0.2, F_W = 0.5, Sc = 0.24$.

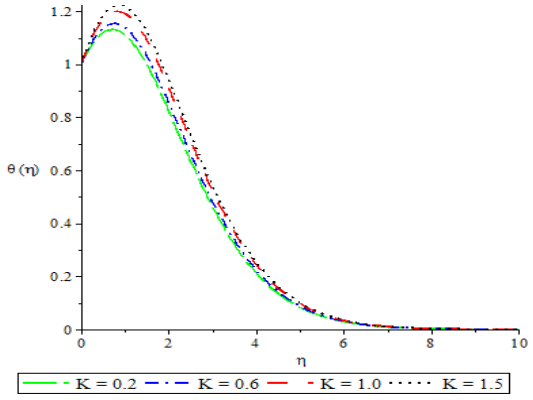

Figure-13. Temperature profiles for
$Pr = 0.72,\ S = 1.0, \varepsilon = 0.05, \lambda_t = 0.5, \lambda_C = 0.5,\ F_W = 0.5, Sc = 0.24$.

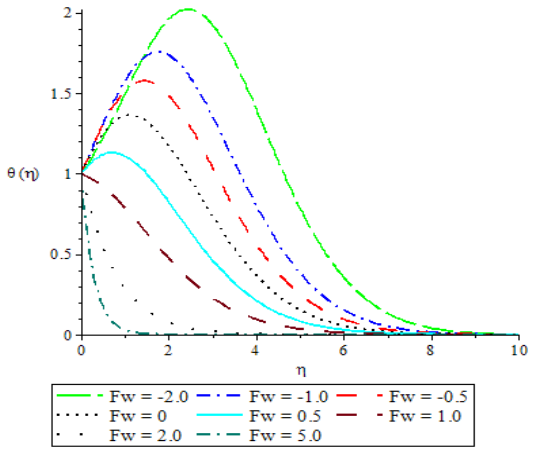

Figure-15. Temperature profiles showing influence of suction/injection for
$Pr = 0.72,\ S = 1.0, \varepsilon = 0.05, \lambda_t = 0.5, \lambda_C = 0.5, K = 0.2, Sc = 0.24$.

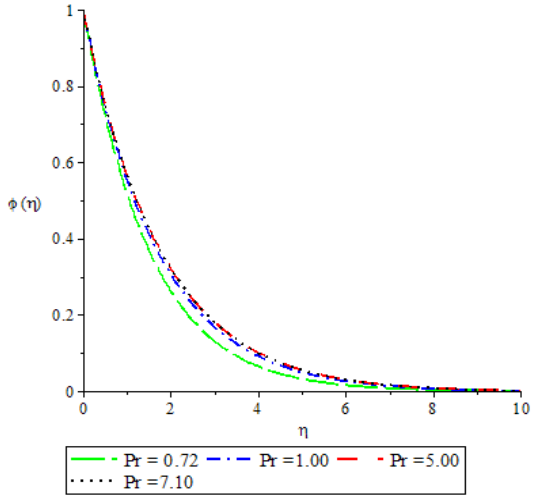

Figure-16. Concentration profiles for
$S = 1.0, \varepsilon = 0.05, \lambda_t = 0.5, \lambda_C = 0.5, K = 0.2, F_W = 0.5, Sc = 0.24$.

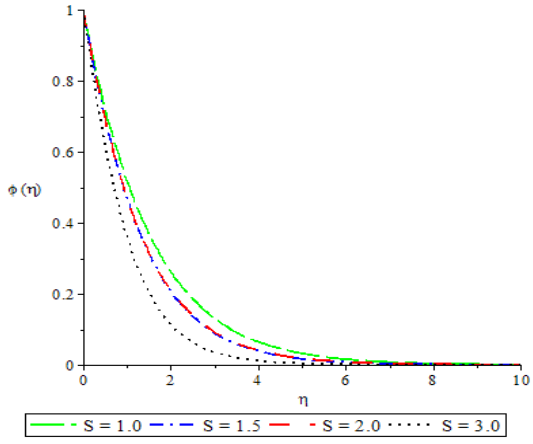

Figure-17. Concentration profiles for
$Pr = 0.72,\ \varepsilon = 0.05, \lambda_t = 0.5, \lambda_C = 0.5, K = 0.2, F_W = 0.5, Sc = 0.24$.

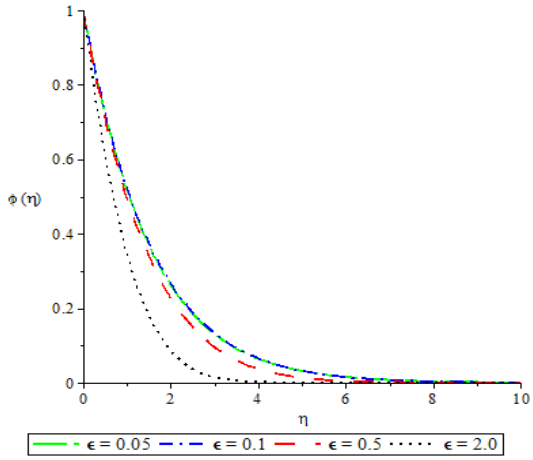

Figure-18. Concentration profiles for
$Pr = 0.72,\ S = 1.0, \lambda_t = 0.5, \lambda_C = 0.5, K = 0.2, F_W = 0.5, Sc = 0.24$.

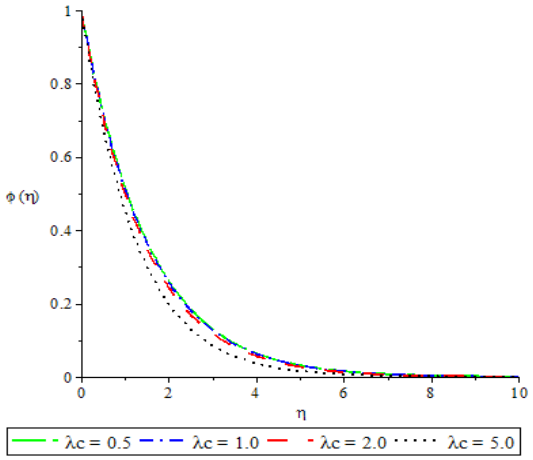

Figure-19. Concentration profiles for $Pr = 0.72,\ S = 1.0, \varepsilon = 0.05, \lambda_t = 0.5, K = 0.2, F_W = 0.5, Sc = 0.24$.

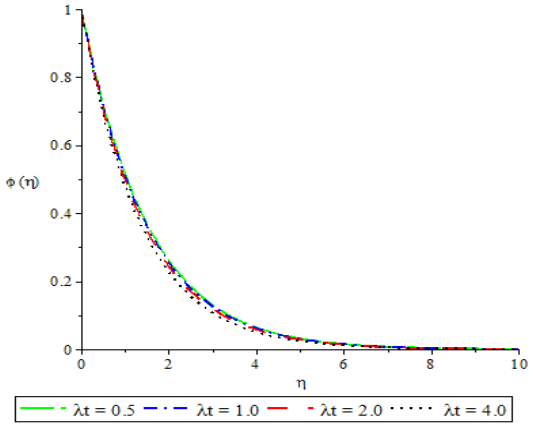

Figure-20. Concentration profiles for $Pr = 0.72,\ S = 1.0, \varepsilon = 0.05,\ \lambda_c = 0.5, K = 0.2, F_W = 0.5, Sc = 0.24$.

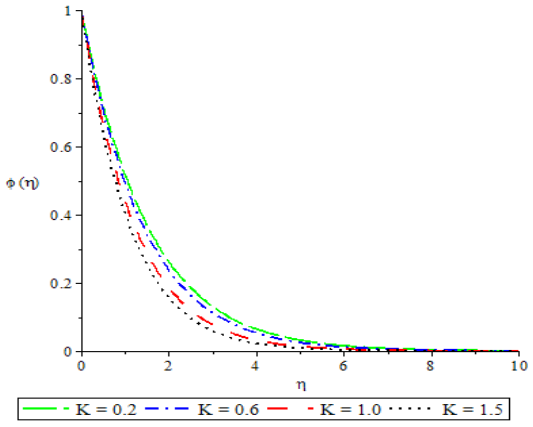

Figure-21. Concentration profiles for $Pr = 0.72,\ S = 1.0, \varepsilon = 0.05, \lambda_t = 0.5, \lambda_c = 0.5,\ F_W = 0.5, Sc = 0.24$.

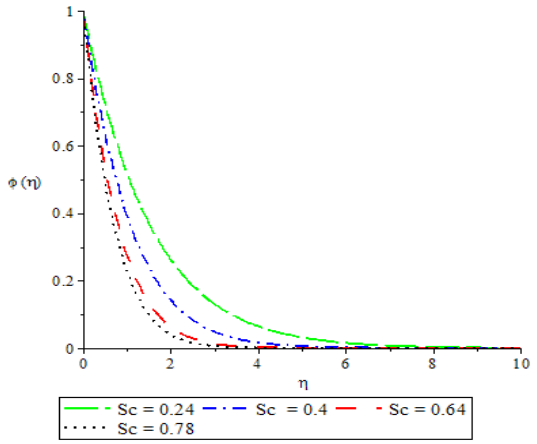

Figure-22. Concentration profiles for $Pr = 0.72,\ S = 1.0, \varepsilon = 0.05, \lambda_t = 0.5, \lambda_c = 0.5,\ K = 0.2, F_W = 0.5$.

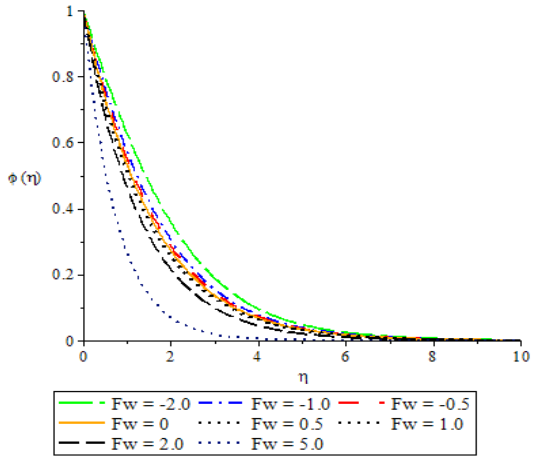

Figure-23. Concentration profiles showing influence of suction/injection for $Pr = 0.72,\ S = 1.0, \varepsilon = 0.05, \lambda_t = 0.5, \lambda_c = 0.5,\ K = 0.2, Sc = 0.24$.

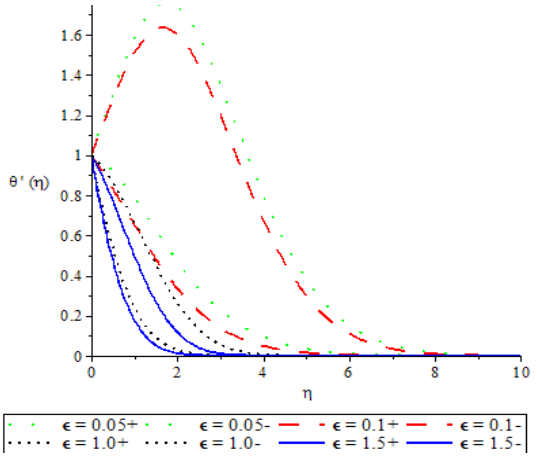

Figure-24. Concentration profiles showing the influence of the velocity ratio and mass transfer $F_W = -\frac{1.0}{1.0}$ for $Pr = 0.72,\ S = 1.0, \lambda_t = 0.5, \lambda_c = 0.5, K = 0.2, Sc = 0.24$.

5. CONCLUSIONS

The steady flow, heat and mass field characteristics of a stretching vertical permeable plate embedded in an incompressible, viscous chemically reacting fluid subject to mixed convection and internal heat generation have been investigated numerically by means of a shooting technique. Our results reveal that each of the governing flow parameters significantly alters all the basic physical quantities as follows:

- skin-friction coefficient at the plate surface grows in intensity as the internal heat generation, suction parameter, thermal and solutal Grashof numbers increase but dwindle in intensity as the injection parameter, Prandtl and Schmidt numbers increase.
- The heat transfer rate at the plate surface in terms of the Nusselt number is enhanced as each of the governing parameters save for injection parameter which exhibits the converse.
- The mass transfer rate at the plate in terms of the Sherwood number is enhanced by increasing variation in the velocity ratio, chemical reaction rate parameter, Schmidt, thermal and solutal Grashof numbers but contrary is the case with an increase in either of the Prandtl number and the internal heat generation.
- An increase in the internal heat generation, the velocity ratio, the thermal and solutal Grashof numbers gives rise to fluid accelerating while the velocity boundary layer becomes thinner but reverse is the case if either the Prandtl number or suction parameter is increased.
- The fluid temperature distribution is higher for the injection as compared with the suction as velocity ratio advances.
- The fluid temperature field dwindles in intensity as the suction parameter, the velocity ratio, the Prandtl, thermal and solutal Grashof numbers each intensifies.
- The species concentration is enhanced by increasing the internal heat generation, chemical reaction rate or the injection parameter but the converse is observed when the suction parameter, the velocity ratio, the Prandtl, thermal and solutal Grashof numbers each intensifies.

AKNOWLEDGEMENTS

The authors would like to appreciate the library, internet access and computer facilities provided by the University of Lagos during the course of this work.

REFERENCES

[1] K. Hiemenz. 1911. Die Grenzschicht an eimen in den gleichformigen Flussignkeitsstrom eingetauchten geraden Kreiszylinder Dingl, Polytech. J. 32: 321-410.

[2] N. Ramachandran, T.S. Chen and B.F. Armaly. 1988. Mixed convection in stagnation flows adjacent to vertical surfaces, ASME J. Heat Transfer. 110: 373-377.

[3] C.D.S Devi, H.S Takhar and G. Nath. 1991. Unsteady mixed convection flow in stagnation region adjacent to a vertical surface, Heat Mass Trans. 26: 71-79.

[4] P.S Gupta and A.S. Gupta. 1977. Heat and mass transfer on a stretching sheet with suction or blowing, Can. J. Chem. Eng. 55: 744-746.

[5] E. Magyari and B. Keller. 2000. Exact solution for self-similar boundary-layers flows induced by permeable stretching surface, Eur. J. Mech B-Fluids. 19: 109-122.

[6] S.Y. Ibrahim and O.D. Makinde. 2010. Chemically reacting MHD boundary layer flow of heat and mass transfer over a moving vertical plate with suction. Scientific Research and Essays. 5(19): 2875-2882.

[7] T.G. Okadayo, Y.M. Aiyesimi, B.I Mundi. 2012. Viscous Dissipation Effect on the Mixed Convention MHD Flow towards a Stagnation Point with Convective Boundary Condition in a Porous medium. Academic Research International, international. 2(2): 184-190.

[8] F. Aman, A. Ishak, I. Pop. 2012. Mixed convection boundary layer flow near stagnation-point on vertical surface with slip, Appl. Math. Mech. Engl. Ed. 32(12): 1599-1606.

[9] O.D. Makinde, P.O. Olanrewaju. 2011. Unsteady mixed convection with Soret and Dufour effects past a porous plate moving through a Binary Mixture of Chemically reaction fluid. Chemical Engineering Communications. 198 (7): 920-938.

[10] O.D. Makinde, P.O. Olanrewaju, W.M. Charles. 2011. Unsteady convection with Chemical reaction and radiative heat transfer past a flat porous plate moving through a binary mixture, Afri. MaT. 22: 65-8.

[11] P.O. Olanrewaju and J.A. Gbadeyan. 2011. Effects of Soret, Dufour, Chemical Reaction, Thermal Radiation and Volumetric Heat Generation/Absorption and a Mixed Convention Stagnation Point Flow on an Isothermal Vertical Plate in Porous Media. The Pacific Journal of Science and Technology [PJST]. 12(2): 234-245.

[12] P.O. Olanrewaju and A. Adeniyan. 2013. Dufour and Soret Effects on MHD Free Convection with Thermal Radiation and Mass Transfer past a Vertical Plate Embedded in a Porous Medium. Nonlinear Sci. Lett. A. 4(1): 21-24.

[13] T.C Chiam. 1994. Stagnation-Point flow towards a stretching plate J. Phys. Sco. Japan. 63: 2443-2444.

[14] A. Ishak, R. Nazar, I. Pop. 2006. Mixed convection boundary layers in the stagnation-point flow toward a tretching vertical sheet, Meccanica. 41: 509-518.

[15] Ishak A., Nazar R., Arifin N.M and Pop I. 2007. Mixed convection of a stagnation point flow towards a stretching permeable sheet. Malaysian journal of Mathematical sciences. 1(2): 217-226, 200.

[16] A. Ridha. 1996. Aiding flows non-unique similarity solutions of mixedconvection boundary-layer equations, Z. Angew Math Phys (ZAMP). 47(3): 341-352.

[17] J.H. Merkin and I. Pop. 2002. Mixed convection along a vertical surface: Similarity solutions for uniform flow. Fluid Dynamics Research. 30(4): 233-250.

[18] F. Aman A, Ishak. 2010. Mixed Convection Flows Toward a Stagnation-point on a Stretching Sheet. Australian Journal of Basic and Applied Sciences. 4(9): 4453-4460.

[19] N. Bachok, A. Ishak, I. Pop. 2013. Mixed Convection Boundary Layer Flow over a Moving Vertical Flat Plate in an External Fluid Flow with Viscous Dissipation Effect. PLoS ONE 8(4): e60766. doi:10.1371/journal.pone.0060766.

[20] O.D. Makinde and P.O. Olanrewaju. 2010. Buoyancy effects on thermal boundary layer over a vertical plate with a convective boundary condition, Journal of Engineering Fluids (ASME). 132: 044502-1-044502-4.

[21] O.D. Makinde, U.S. Mahebaleswar, N. Maheshkumar. 2013. Non-perturbative Solution for Hydro magnetic Flow over a Linearly Stretching Sheet, Int. J. of Applied Mechanics and Engineering. 18(3): 935-943.